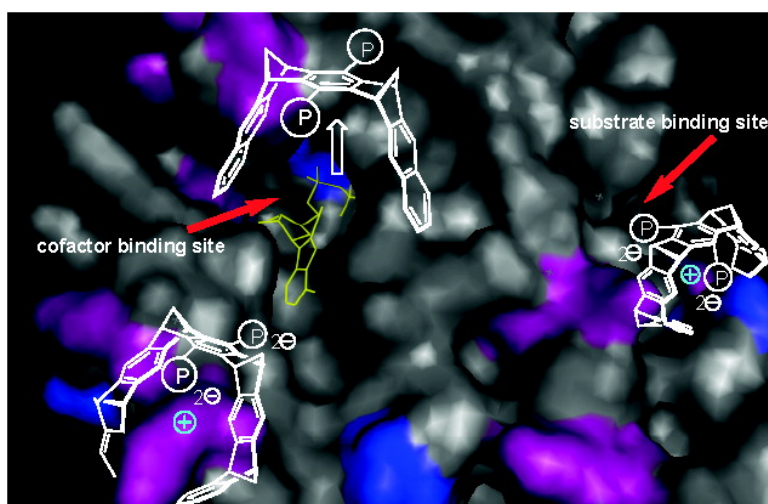


## Molecular Clip and Tweezer Introduce New Mechanisms of Enzyme Inhibition

Peter Talbiersky, Frank Bastkowski, Frank-Gerrit Klärner, and Thomas Schrader

*J. Am. Chem. Soc.*, **2008**, 130 (30), 9824-9828 • DOI: 10.1021/ja801441j • Publication Date (Web): 08 July 2008

Downloaded from <http://pubs.acs.org> on February 8, 2009



### More About This Article

Additional resources and features associated with this article are available within the HTML version:

- Supporting Information
- Links to the 1 articles that cite this article, as of the time of this article download
- Access to high resolution figures
- Links to articles and content related to this article
- Copyright permission to reproduce figures and/or text from this article

[View the Full Text HTML](#)

## Molecular Clip and Tweezer Introduce New Mechanisms of Enzyme Inhibition

Peter Talbiersky, Frank Bastkowski, Frank-Gerrit Klärner, and Thomas Schrader\*

Department of Chemistry, University Duisburg-Essen, Universitätsstrasse 5,  
45117 Essen, Germany

Received February 26, 2008; E-mail: Thomas.Schrader@uni-due.de

**Abstract:** Artificial molecular clips and tweezers, designed for cofactor and amino acid recognition, are able to inhibit the enzymatic activity of alcohol dehydrogenase (ADH).  $IC_{50}$  values and kinetic investigations point to two different new mechanisms of interference with the  $NAD^+$ -dependent oxidoreductase: While the clip seems to pull the cofactor out of its cleft, the tweezer docks onto lysine residues around the active site. Both modes of action can be reverted to some extent, by appropriate additives. However, while cofactor depletion by clip **1** was in part restored by subsequent  $NAD^+$  addition, the tweezer (**2**) inhibition requires the competitive action of lysine derivatives. Lineweaver–Burk plots indicate a competitive mechanism for the clip, with respect to both substrate and cofactor, while the tweezer clearly follows a noncompetitive mechanism. Conformational analysis by CD spectroscopy demonstrates significant ADH denaturation in both cases. However, only the latter case (tweezer–lysine) is reversible, in full agreement with the above-detailed enzyme switch experiments. The complexes of ADH with clips or tweezer can be visualized in a nondenaturing gel electrophoresis, where the complexes migrate toward the anode, in contrast to the pure enzyme which approaches the cathode. Supramolecular chemistry has thus been employed as a means to control protein function—with the specificity of artificial hosts opening new avenues for this endeavor.

### Introduction

For a selective shut-down of pathological protein functions, medicinal chemistry has developed efficient ways to design small ligands for the natural binding sites.<sup>1</sup> X-ray crystallography, combinatorial screening, and molecule modeling finally culminate in the construction of synthetic molecules, which perfectly fit into the cleft of the natural compound and thus block the respective protein, for example, a strategic receptor.<sup>2</sup> Supramolecular chemistry has in the past decades learned from natural recognition processes and gained a deeper understanding of the crucial factors governing molecular recognition in water.<sup>3</sup> Systematic investigations on model compounds with a focus on energy balances and stereoelectronic factors have produced new approaches to achieve desolvation of essential biomolecules and host–guest binding, at physiological conditions.<sup>4</sup> It is time to test artificial host molecules in biological systems.<sup>5</sup>

The Klärner group has devised molecular clips and tweezers which offer a highly electron-rich interior and are potent hosts

for electron-poor (hetero)aromatics such as pyridinium salts.<sup>6</sup> Attachment of two phosphate groups to their periphery renders these hosts water-soluble and produces artificial receptor molecules which operate in water.<sup>7</sup> If the polar center piece carries two planar aromatic side walls (most often naphthalene moieties), so-called molecular clips are formed which preferentially draw aromatic cofactor molecules into their narrow cavity—such as nicotinamide adenine dinucleotide ( $NAD^+$ ), thiamine diphosphate (TPP), and *S*-adenosylmethionine (SAM).<sup>8</sup> If the side walls are kinked (as, e.g., in dibenzonorbornadienes), the endo selectivity of the critical Diels–Alder step leads to a molecular tweezer with a torus-shaped overall structure embracing an almost centroid inner cavity.<sup>9</sup> These tweezers are selective for lysine and, to a lesser degree, arginine residues (Figure 1).<sup>10</sup>

Here we report on the effect of the phosphate-substituted clip **1** and tweezer **2** on the enzymatic oxidation of ethanol catalyzed by alcohol dehydrogenase (ADH) using  $NAD^+$  as cofactor. The hitherto unknown tweezer **2** was prepared analogously to clip

- (1) (a) Nogrady, T.; Weaver, D. F. *Medicinal Chemistry - A Molecular and Biochemical Approach*; Oxford University Press: New York, 2005. (b) *Wilson & Gisvold's Textbook of Organic Medicinal and Pharmaceutical Chemistry*; Block, J., Beale, J. M., Eds.; Lippincott Williams & Wilkins: Philadelphia, PA, 2003.
- (2) (a) *Molecular Modeling: Basic Principles and Applications*; Höltje, H.-D., Sippl, W., Rognan, D., Folkers, G., Eds.; Wiley-VCH: Weinheim, Germany, 2003. (b) *Protein Crystallography in Drug Discovery*; Babine R. E., Abdel-Meguid S. S., Eds.; Wiley-VCH: Weinheim, Germany, 2004.
- (3) Meyer, E. A.; Castellano, R. K.; Diederich, F. *Angew. Chem., Int. Ed.* **2003**, *42*, 1210–1250.
- (4) Oshovsky, G. V.; Reinhoudt, D. N.; Verboom, W. *Angew. Chem., Int. Ed.* **2007**, *46*, 2366–2393.

- (5) (a) Bell, T. W.; Lin, Q.; Park, H. S.; Hamuro, Y.; Loe, C. S.; Hamilton, A. D. *Peptide Science* **1999**, *47*, 285–297. (b) You, C.-C.; De, M.; Rotello, V. M. *J. Am. Chem. Soc.* **2005**, *127*, 12873–12881. (c) Schulze, K.; Mulder, A.; Tinazli, A.; Tampé, R. *Angew. Chem., Int. Ed.* **2006**, *45*, 5702–5705.
- (6) Klärner, F.-G.; Kahlert, B. *Acc. Chem. Res.* **2003**, *36*, 919–932.
- (7) Jasper, C.; Schrader, T.; Panitzky, J.; Klärner, F.-G. *Angew. Chem., Int. Ed.* **2002**, *41*, 1355–1358.
- (8) (a) Fokkens, M.; Jasper, C.; Schrader, T.; Koziol, F.; Ochsenfeld, C.; Polkowska, J.; Lobert, M.; Kahlert, B.; Klärner, F.-G. *Chem. Eur. J.* **2005**, *11*, 477–494. (b) Schrader, T.; Fokkens, M.; Klärner, F.-G.; Polkowska, J.; Bastkowski, F. *J. Org. Chem.* **2005**, *70*, 10227–10237.
- (9) Klärner, F.-G.; Burkert, U.; Kamieth, M.; Boese, R.; Benet-Buchholz, J. *Chem.—Eur. J.* **1999**, *5*, 1700–1707.
- (10) Fokkens, M.; Schrader, T.; Klärner, F.-G. *J. Am. Chem. Soc.* **2005**, *127*, 14415–14421.

**1**<sup>8a</sup> starting from the corresponding hydroquinone tweezer **2** (OH instead of  $\text{OPO}_3^{2-} 2\text{Li}^+$ )<sup>9</sup> <sup>1</sup>H NMR as well as fluorescence titrations in buffered aqueous solution furnished  $K_D$  values for the phosphates in the micromolar range (**1**· $\text{NAD}^+$ : 141  $\mu\text{M}$ ; **2**·lysine (AcLysOMe·AcOH): 20  $\mu\text{M}$ ). The phosphate-substituted tweezer **2** binds lysine substantially stronger by a factor of 13 than does the corresponding phosphonate-substituted tweezer **2** ( $\text{OP}(\text{Me})\text{O}^{2-} \text{Li}^+$  instead of  $\text{OPO}_3^{2-} 2\text{Li}^+$ ),<sup>10</sup> whereas the difference in the binding of  $\text{NAD}^+$  by the phosphate- and phosphonate-substituted clip **1** is small.

A large and well-known family of  $\text{NAD}^+$ -dependent enzymes oxidizes simple hydroxylic substrates, the alcohol dehydrogenases (ADH).<sup>11</sup> These display at the same time multiple lysines and arginines on their protein surfaces, some of them even located in the vicinity of the active site, which render the whole protein basic ( $\text{pI} \approx 8$ ).<sup>12</sup> A powerful noncovalent interaction between the cofactor embedded in the Rossman-fold<sup>13</sup> with an externally added  $\text{NAD}^+$ -“trap” might deplete the cofactor level below the critical threshold and severely impede the enzymatic alcohol oxidation. Likewise, complexation of lysine and arginine residues around the entrance to the cofactor cleft or the substrate binding site by a tweezer molecule should have a significant influence on enzymatic activity.

We therefore chose a standard ADH assay with ethanol serving as the substrate, which is oxidized to acetaldehyde.<sup>14</sup> This assay requires a large excess of  $\text{NAD}^+$  for reliable substrate conversion, which is in turn measured indirectly by the rise in NADH, producing a distinct extinction increase at 340 nm in the UV/vis spectrum. ADH was taken from baker's yeast (*Saccharomyces cerevisiae*); like all dehydrogenases this is a bireactant system, operating with two separate binding sites for cofactor and substrate.<sup>15</sup> This ADH binds its oxidized cofactor only weakly ( $\text{ADH} \cdot \text{NAD}^+$ : 610  $\mu\text{M}$ ), so that an external competitor has a genuine chance to interfere.<sup>14</sup> It is well-known, that ADH is kinetically characterized by a typical C-NC-UC-C scheme (C, competitive; NC, noncompetitive; UC, uncompetitive), classifying the enzyme as a “steady-state, sequential ordered” system.<sup>15</sup> Hence, both binding sites accommodate their respective guests in a rapid equilibrium, but cofactor addition must come first, since it induces a conformational change, closes the Rossman fold, and opens the substrate binding site for optimal hydride transfer.

## Results and Discussion

A systematic investigation of enzyme velocity vs incrementally increased clip concentration revealed a strong correlation, with high  $\text{IC}_{50}$  values of 1.5 mM for phosphate clip **1**. This high number, however, originates from the large cofactor excess

and thus has to be compared with the initial  $\text{NAD}^+$  concentration of 1.8 mM. A more appropriate expression would result from calculating the inhibitor/cofactor ratio, which is 0.8 equivalents of clip **1**. Thus, substoichiometric amounts of the phosphate clip suffice to block ADH by 50%.

Lineweaver–Burk plots (shown in the Supporting Information), obtained from the analysis of the reaction rate in dependence of the substrate and cofactor concentration, clearly revealed that clip **1** competes with cofactor binding, but not with substrate recognition. Only infinite cofactor concentrations lead to a fully restored native enzyme activity (intersection of both lines on the y-axis of the plot). Such a competitive inhibition supports the  $\text{NAD}^+$  depletion mechanism; it could, however, also vote for a direct docking mechanism of the clip into the cofactor cleft, most likely opposite to the catalytically active site where the substrate is processed. A close inspection of crystal structures confirms the accessibility of this remote part of the cofactor binding cleft, which is also surrounded by several basic amino acids.<sup>16</sup>

A putative protein-clip complex could be identified after 1 h of native gel-electrophoresis; however, after 2 h, it had split up and the free clip migrated toward the anode, in contrast to the pure slightly basic enzyme, which approached the cathode (see Supporting Information).<sup>17</sup> To check the postulated inhibition by  $\text{NAD}^+$  depletion, 2 equiv of the cofactor were added onto the assay containing inhibitor **1**. Enzymatic substrate oxidation was markedly accelerated, although it never reached the original (native) value. Surprisingly, no beneficial effect was achieved by external addition of a superior guest for clip **1** (*N*-methylnicotinamide iodide (NMNA)/ $K_D = 30 \mu\text{M}$ ). This may indicate a partial denaturation or a highly stable ternary complex between enzyme, cofactor, and clip. It might be argued that NMNA acts as a  $\text{NAD}^+$  mimic and blocks the Rossman fold.<sup>18</sup> However, its equimolar presence did not influence the normal assay, nor could NMNA alone catalyze the oxidation reaction (see Supporting Information). CD spectroscopy of the enzyme with cofactor and its complex with the clip shed new light on the mechanism of inhibition.<sup>19</sup> In the clip complex of ADH, the negative ellipticity increase at 220 nm is markedly lowered compared to that of pure ADH and cannot be restored even by the addition of a 10-fold excess of cofactor  $\text{NAD}^+$ , pointing to a substantial amount of irreversible denaturation (Figure 2).<sup>20</sup>

We conclude, that clip **1** most likely operates with a dual mechanism. Only after 63% inhibition with **1**,  $\text{NAD}^+$  was able to fully restore enzymatic activity. If **1** was added in 10-fold excess so that the enzyme was completely shut down, it could not be “turned on” again. All these observations, together with the CD results point toward a combination of cofactor trapping with a partially irreversible inhibition by enzyme denaturation. Prior to any efficient cofactor action, a conformational flip must occur in the parent enzyme after  $\text{NAD}^+$  binding, bringing the pyridinium ring and the substrate in close proximity.<sup>21</sup> This

- (11) (a) Dickinson, F. M.; Monger, G. P. *Biochem. J.* **1973**, *131*, 261–270. (b) Schöpp, W.; Aurich, H. *Biochem. J.* **1976**, *157*, 15–22. (c) Ganzhorn, A. J.; Green, D. W.; Hershey, A. D.; Gould, R. M.; Plapp, B. V. *Biol. Chem.* **1987**, *262*, 3754–3761. (d) Leskovic, V.; Trivic, S. *Biochem. Mol. Biol. Int.* **1994**, *32*, 399–407. (e) Leskovic, V. *FEMS Yeast Res.* **2002**, *481–494*.
- (12) These basic amino acid residues are utilized inter alia for the appropriate placement of the cofactor's phosphodiester anions in the cleft.
- (13) Rossmann, M. G.; Moras, D.; Olsen, K. W. *Nature* **1974**, *250*, 194–199.
- (14) Bergmeyer H. U.; Bergmeyer, J. Grassl, M. *Samples, Reagents, Assessment of Results; Methods of Enzymatic Analysis*, 3rd ed., Vol. 2; Verlag Chemie: Weinheim, Germany, 1983.
- (15) Taylor, K. B. *Effects of Analogue Inhibitors. Enzyme Kinetics and Mechanisms*; Kluwer Academic Publishers: Dordrecht, The Netherlands, 2002; Chapter 6.

- (16) RCSB protein data bank 1PS0: (a) Valencia, E.; Larroy, C.; Ochoa, W. F.; Parés, X.; Fita, I.; Biosca, J. A. *J. Mol. Biol.* **2004**, *341*, 1049–1062. (b) 2HCY: Plapp, B. V., Savarimuthu, B. R., Subramanian.
- (17) McKinley-McKee, J. S.; Moss, D. W. *Biochem. J.* **1965**, *96*, 583.
- (18) Lo, H. C.; Fish, R. H. *Angew. Chem., Int. Ed.* **2002**, *41*, 478–481.
- (19) Creagh, A. L.; Prausnitz, J. M.; Blanch, H. W. *Biotechnol. Bioeng.* **2007**, *41*, 156–161.
- (20) Tagore, D. M.; Sprinz, K. I.; Fletcher, S.; Jayawickramarajah, J.; Hamilton, A. D. *Angew. Chem., Int. Ed.* **2007**, *46*, 223–225. (a) An alternative explanation involving a tight clip-protein complex cannot be entirely ruled out.
- (21) Exequiel, J. R.; Pineda, T.; Callender, R.; Schwartz, S. D. *Biophys. J.* **2007**, *93*, 1677–1686.

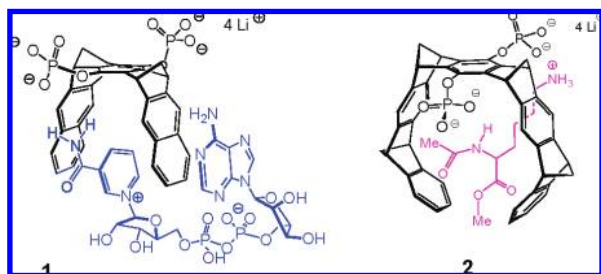


**Figure 1.** Phosphate clip **1** with complexed  $\text{NAD}^+$  (left) and phosphate tweezer **2** with included lysine (right); Lewis structures drawn from calculations (MacroModel 8.1, 5000 steps, water, Amber\*).

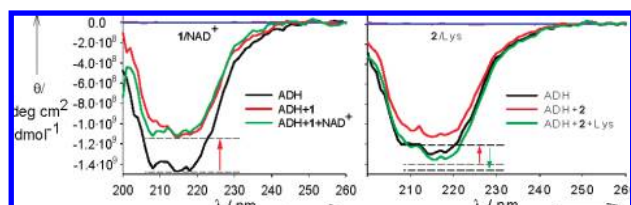


**Figure 2.** CD spectra of pure ADH ( $10^{-7}$  M) and its complex with **1** or **2** ( $10^{-6}$  M) as well as with additional  $\text{NAD}^+$  or Ac-Lys-OMe ( $10^{-5}$  M).

conformational flexibility may be lost after clip **1** has docked onto the ADH molecule.

Although the tweezer **2** hardly binds  $\text{NAD}^+$  ( $K_D \approx 0.5$  mM), it shuts down ADH much more efficiently than the related clip **1**. The  $\text{IC}_{50}$  value (determined under the same conditions as that of clip **1**) amounts to only 0.09 equivalents of  $\text{NAD}^+$  (180  $\mu\text{M}$ ). Clearly, **2** cannot act as an  $\text{NAD}^+$  trap in this case. Intriguingly, the conformationally closed Rossman fold formed after cofactor binding displays two entrance holes, one of which hosts the nicotinamide and is therefore located close to the substrate binding site; this is surrounded by several arginine residues. The opposite side with the adenine moiety is surrounded by multiple lysines.<sup>16</sup> An alternative explanation for the tweezer's high efficiency in enzyme inhibition is a selective complexation of these lysine residues by tweezer molecules, which either distort or directly block the entrance of the cofactor binding site. If this is the case, subsequent  $\text{NAD}^+$  addition should have no beneficial effect on enzyme recovery. On the contrary, addition of a lysine derivative (forming a stable host–guest complex with tweezer **2**) should allow for a mild detachment of the tweezer molecules from strategically placed lysine residues around the Rossman fold entrance. Both hypotheses were indeed experimentally verified with a partially blocked enzyme at the  $\text{IC}_{50}$  point: While even 5 equiv of  $\text{NAD}^+$  have no effect, the addition of Ac-Lys-OMe (2 equiv) restores 74% of the original enzyme activity and peptide H-KKKK-OH restores even 89%. Figure 3 shows a successful ADH switch experiment: 0.6 equiv of tweezer **2** (related to  $\text{NAD}^+$ ) stops all enzyme activity, reverts by 3 equiv of Ac-Lys-OMe to about 40% of original activity, and finally totally shuts down again by 2.4 equiv of **2**. These results allow the conclusion that the complexation of the enzyme lysine residues by tweezer **2** is reversible and the equilibrium can be shifted toward the free enzyme by addition of external lysine derivatives. This is not possible if ADH reacts with clip **1**, since the addition of NMNA as an efficient clip binder has no effect.

Strong experimental evidence for this new type of enzyme inhibition comes from detailed recovery experiments which correlate the ability of representative amino acids to restore enzyme function with their respective affinity toward tweezer

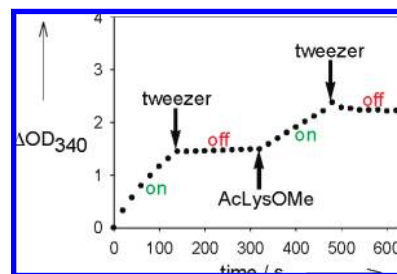


**Figure 3.** Enzyme switching: external alternating addition of tweezer and lysine turns enzyme activity on and off (ADH  $10^{-7}$  M, phosphate buffer).

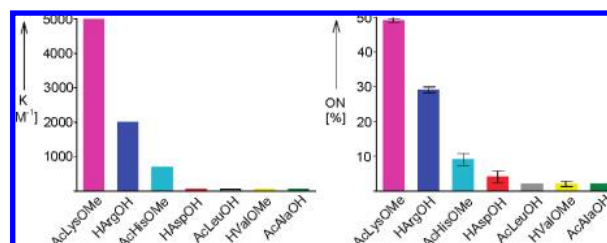


**Figure 4.** (left) Relative affinities of representative amino acids toward bisphosphonate tweezer **2a** in aqueous buffer. (right) Relative recovery effects of selected amino acids on restored ADH activity after total inhibition by **2**.

**2**. After total enzyme shut-down by **2**, seven basic, acidic, and unpolar amino acid derivatives (3 equiv) were added and displayed a recovery rate that reflected their relative affinities toward the related bisphosphonate derivative **2a** (Figure 4).

It might be argued that clip and tweezer could potentially also exert their inhibitory effect on ADH by nonspecific electrostatic interactions with basic amino acid residues on the protein surface. To investigate the influence of this aromatic diphosphate moiety both clip and tweezer were stripped of their sidewalls and the remaining centerpiece was synthesized and tested in the above-delineated enzyme assay. No inhibition was detectable nor could any  $\text{IC}_{50}$  value be determined. This direct comparison proves that the clip and tweezer sidewalls are essential for their biological effect—a strong indication for the inclusion of specific guest moieties inside their cavities, which differ in size and shape.

Enzyme kinetics further support these conclusions: the inhibition by tweezer **2** is noncompetitive with respect to both substrate and cofactor binding sites. The two lines (representing the enzymatic reactions undisturbed and disturbed by tweezer **2**) intersect in the negative part of the  $x$ -axis of the Lineweaver–Burk plot (see Supporting Information).

In the CD spectrum of ADH (carbonyl region 200–250 nm) significant changes occur on tweezer binding, which are, however, fully reversible after addition of Ac-Lys-OMe (Figure 2). Obviously, lysine complexation is accompanied with a conformational change within the ADH surface. After external addition of lysine derivatives, however, this noncovalent denaturation is fully canceled, as evidenced by the restored CD spectrum of native ADH. A final piece of evidence comes from native gel electrophoresis. Even a large excess of negatively charged tweezer molecules (anode) is totally absorbed by the slightly basic protein (cathode); thus a new spot is produced for the complex, which migrates after 1 h only marginally, but

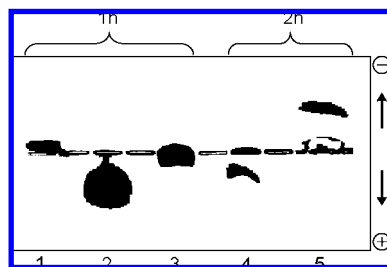


**Figure 5.** Nondenaturing gel electrophoresis on agarose showing the weakly basic protein being attracted by the cathode (2 h), whereas the oppositely charged tweezer migrates toward the anode (1 h). Complex formation results in an intermediate migration behavior (1 h, 2 h): (1) ADH; (2) tweezer 2; (3) ADH + tweezer 2; (4) ADH + tweezer 2; (5) ADH.

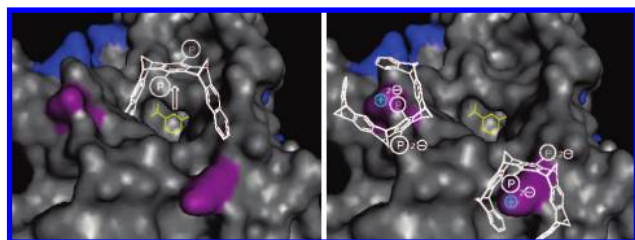


**Figure 6.** Entry to the Rossman fold and divergent inhibition mechanisms of clip 1 and tweezer 2: While the clip pulls out the cofactor (yellow), the tweezer decorates the surrounding lysine residues. Crystal structure 1PS0 (ADH from *Saccharomyces cerevisiae*) from the protein data bank; arg = blue, lys = purple.

after 2 h clearly toward the anode due to charge overcompensation on ADH's protein surface (Figure 5).

## Conclusion and Outlook

Two artificial water-soluble host molecules were shown to block the enzymatic oxidation of ethanol by ADH *in vitro*. Their substrate specificity dictates two different ways to reach the same goal: clip 1 pulls out  $\text{NAD}^+$  from the Rossman fold and thereby depletes the cofactor level below a critical threshold. It may also be able to bind nonspecifically to the enzyme, most likely to basic domains and the empty Rossman fold, leading to irreversible denaturation. Tweezer 2 with its high lysine preference decorates the whole enzyme surface, especially the cofactor entrance site. This much more efficient process, however, results in a reversible conformational change, as evidenced by enzyme switching experiments and CD investigations (Figure 6).

A comparative experiment in 50 mM phosphate buffer with an additional 250 mM NaCl salt load reflected the superior inhibitory power of tweezer 2: While the absolute enzymatic activity was not influenced at all, 0.6 equiv of tweezer were still sufficient for a total enzyme shut down, whereas the same amount of clip 1 did only slow down the ethanol oxidation by 40%. Thus, the increased ionic strength weakens  $\text{NAD}^+$  inclusion and nonspecific clip-adhesion to the enzyme surface, but has little effect on lysine recognition by tweezer 2—another piece of experimental evidence for strong contributions of aromatic  $\pi$ -cation interactions in this specific binding mechanism.<sup>22</sup>

This work demonstrates how the guest specificity of artificial host molecules is retained in the biological environment of

protein recognition. The results hold promise to selectively target proteins with specific critical amino acid residues. In our case, we will look for enzymes whose biological function relies on single strategic lysine residues. In the future, we will also examine other representatives of the large family of  $\text{NAD}^+$ -dependent enzymes. Control over protein function could have beneficial effects on  $\text{NAD}^+$ -driven processes involving, *inter alia*, DNA ligation, ADP ribosylation, or NAD phosphorylation.<sup>23</sup>

## Experimental Section

**Tetra(lithium)-(5 $\alpha$ ,7 $\alpha$ ,9 $\alpha$ ,11 $\alpha$ ,16 $\alpha$ ,18 $\alpha$ ,20 $\alpha$ ,22 $\alpha$ )-5,7,9,11,16,18,20,22-octahydro-5,22:7,20:9,18:11,16-tetramethanononacene-8,19-bis-phosphate 2.** The synthesis of tweezer 2 followed the procedure reported for the preparation of clip 1.<sup>8b</sup> The stirred solution of hydroquinone tweezer 2 (OH instead of  $\text{OPO}_3^{2-} 2 \text{Li}^+$ ) (0.35 mmol) in anhydrous THF (20 mL) was treated at 0 °C with phosphoroylchloride (0.70 mmol) and triethylamine (0.80 mmol). After the usual workup the free phosphoric acid derivative 2 ( $\text{OPO}_3\text{H}_2$  instead of  $\text{OPO}_3^{2-} 2 \text{Li}^+$ ) was precipitated with aqueous HCl and neutralized with lithium hydroxide in methanol to furnish 2 as a white solid (0.28 mmol, 79% over two steps). Decomposition point >200 °C.  $^1\text{H}$  NMR (500 MHz,  $\text{D}_2\text{O}$ ):  $\delta$  = 2.27 (dt, 2 H, 2J(24a-H, 24i-H) = 7.8 Hz, 24a-H, 25a-H), 2.35–2.41 (m, 4 H, 23i-H, 23a-H, 26i-H, 26a-H), 2.55 (dt, 2 H, 24i-H, 25i-H), 4.19 (t, 4 H, 5-H, 11-H, 16-H, 22-H), 4.53 (t, 4 H, 7-H, 9-H, 18-H, 20-H), 6.71 (s(br), 4 H, 2-H, 3-H, 13-H, 14-H), 7.12 (m, 4 H, 1-H, 4-H, 12-H, 15-H), 7.30 ppm (s, 4 H, 6-H, 10-H, 17-H, 21-H).  $^{31}\text{P}$  NMR (202 MHz,  $\text{D}_2\text{O}$ ):  $\delta$  = 0.99 ppm (s,  $\text{OP}(\text{O})(\text{O}^- \text{Li}^+)_2$ ).  $^{13}\text{C}$  NMR (126 MHz,  $\text{D}_2\text{O}$ ):  $\delta$  = 48.22 (d, C-7, C-9, C-18, C-20), 50.76 (d, C-5, C-11, C-16, C-22), 68.13, 68.79 (2 t, C-23, C-24, C-25, C-26), 116.45 (d, C-6, C-10, C-17, C-21), 120.04 (d, C-1, C-4, C-12, C-15), 121.33 (d, C-2, C-3, C-13, C-14), 138.34 (m, C-8, C-19), 141.63 (s, C-7a, C-8a, C-18a, C-19a), 147.75, 148.88 (2 s, C-5a, C-6a, C-9a, C-10a, C-16a, C-17a, C-20a, C-21a), 151.04 ppm (s, C-4a, C-11a, C-15a, C-22a). IR (KBr): $\nu$ [ $\text{cm}^{-1}$ ] = 3065 (C–H), 2975 (C–H), 2938 (C–H), 2865 (C–H), 1467 (C–H), 1281 ( $\text{P}=\text{O}$ ); UV/vis (MeOH):  $\lambda_{\text{max}}$  (lg  $\epsilon$ ) = 208 (4.81), 284 nm (4.02); MS (ESI, MeOH)  $m/z$ : 362 [ $\text{M} - 4 \text{Li} + 2 \text{H}$ ] $^{2-}$ . HRMS for  $(\text{C}_{42}\text{H}_{30}\text{O}_8\text{P}_2)_2$ : calcd, 362.071; found, 362.071.

**Fluorescence Titrations.** In a fluorimeter, tweezer 2 was excited at 280 nm, its emission monitored from 300 to 600 nm. In the host–guest-experiment, which was conducted in 100 mM sodium phosphate buffer (pH 7.7 or pH 9.0) in a quartz cuvette, 700  $\mu\text{L}$  of the host solution were placed in the cuvette and the guest solution was added stepwise. Emission intensity changes were recorded and used in a standard nonlinear regression algorithm to calculate the appropriate association constants.

**Enzyme Activity Assay. (a)  $\text{IC}_{50}$  Values.** All ADH activity assays were performed in microplates in sodium phosphate/glycine buffer (75 mM/22.2 mM, pH 9.0) with  $[\text{GSH}] = 300 \text{ mM}$ ,  $[\text{semicarbazid}] = 2.2 \text{ M}$ ,  $[\text{BSA}] = 1 \text{ mg/mL}$ ,  $[\text{NAD}^+] = 27.7 \text{ mM}$ ,  $[\text{ADH}] = 208 \text{ nM}$ , either  $[\text{clip 1}] = 277 \text{ mM} - 34.6 \mu\text{M}$  or  $[\text{tweezer 2}] = 69.3 \text{ mM} - 34.6 \mu\text{M}$ . A 10  $\mu\text{L}$  portion of one of the two inhibitors was added to a mixture of 178.5  $\mu\text{L}$  buffer, 7.5  $\mu\text{L}$  semicarbazid, 7.5  $\mu\text{L}$  GSH, 16.5  $\mu\text{L}$   $\text{NAD}^+$ , 20  $\mu\text{L}$  ADH, and 10  $\mu\text{L}$  ethanol/buffer (1.18 mg/mL). The ADH activity was observed by monitoring the mOD change at 340 nm over a period of 10 min. From a  $[\text{inhibitor}]/v_0$  plot (inhibitor concentration vs initial enzyme velocity)  $\text{IC}_{50}$  values were determined at half-maximum  $v_0$ . All experiments were performed in triplicate.

**(b) Michaelis–Menten Kinetics.** For Michaelis–Menten kinetics the inhibitor concentrations were kept constant at 1.2 mM for the clip 1 and 232  $\mu\text{M}$  for the tweezer 2, whereas the substrate

(22) Even in the presence 250 mM NaCl the lysine tweezer complex was not sufficiently weakened for enzyme recovery.

(23) (a) Lin, S. J.; Guarente, L. *Curr. Opin. Cell Biol.* **2003**, *15*, 241–246. (b) Pollak, N.; Dölle, C.; Ziegler, M. *Biochem. J.* **2007**, *402*, 205–218.

concentrations were varied. Since ADH is a protein consisting of two substrates, ethanol and  $\text{NAD}^+$ , two cases had to be investigated. In the first case the ethanol concentration was varied from 17 to 170 mM, while the  $\text{NAD}^+$  concentration was kept constant at 1.83 mM. In the second case the  $\text{NAD}^+$  concentration was varied from 0.33 to 7.06 mM, while the ethanol concentration was kept constant at 26 mM. The inhibition mode was determined from a Lineweaver–Burk plot, that is,  $1/[\text{substrate}]$  versus  $1/v_0$ . To find out the enzymatic model ADH follows, both substrates were replaced by analogue inhibitors, 1-butanol for ethanol and  $\text{SNAD}^+$  for  $\text{NAD}^+$ . The received Lineweaver–Burk plots show that ADH follows the steady-state sequential ordered model. All experiments were performed in triplicate.

**Enzyme Switching.** ADH switching was performed by adding to a running enzymatic reaction one of the two inhibitors and its corresponding competing molecule in alternating order. For clip **1** the corresponding competitor was  $\text{NAD}^+$  and for tweezer **2** AcLysOMe was the suitable competing compound. Specifically, the above-described ADH assay was stopped after 2 min by external addition of a 1.05 mM tweezer **2** solution (10  $\mu\text{L}$ , 0.6 equiv toward  $\text{NAD}^+$ ). After another 2 min, a 4.96 mM AcLysOMe solution (10  $\mu\text{L}$ , 3 equiv) was injected and the restored ADH assay was monitored for 2 min. Finally, the enzymatic reaction was again brought to a halt by the addition of 2.4 equiv of tweezer **2**.

**Nondenaturing Gel Electrophoresis.** Agarose gels (1%) for native gel electrophoresis were prepared in 5 mM sodium phosphate buffer (pH 7.0). Wells were formed by placing a comb in the middle of the gel rack for 33  $\mu\text{L}$  samples. The samples contained 30  $\mu\text{L}$  of ADH (191  $\mu\text{M}$ ) and 3  $\mu\text{L}$  of Xylenecyanol+Ficoll-400, 30  $\mu\text{L}$

of tweezer **2** (66.4 mM) and 3  $\mu\text{L}$  of Xylenecyanol+Ficoll-400, and 15  $\mu\text{L}$  of tweezer **2** (33.2 mM), 15  $\mu\text{L}$  of ADH (95.5  $\mu\text{M}$ ), and 3  $\mu\text{L}$  of Xylenecyanol+Ficoll-400. They were incubated for 1 h at ambient temperature and subsequently separated at 35 mA for 1 h and for 2 h. The gels were stained for 15 min with 0.5% Coomassie blue, 40% methanol, and 10% acetic acid aqueous solution and destained with water overnight. When bands were clearly visible, the gels were scanned on a flatbed scanner. All experiments were performed in triplicate.

**CD Spectroscopy.** CD experiments were conducted in a quartz cuvette in 100 mM sodium phosphate buffer (pH 7.69). The samples containing [tweezer **2**] = 1  $\mu\text{M}$ , [clip **1**] = 1  $\mu\text{M}$ , [ADH] = 100 nM, [ $\text{NAD}^+$ ] = 10  $\mu\text{M}$ , and [AcLysOMe] = 10  $\mu\text{M}$  were scanned from 200 to 300 nm at a constant temperature of 25 °C. All experiments were performed in triplicate.

**Acknowledgment.** We wish to thank the group of Prof. Haberhauer, Essen, for measuring all CD spectra. We thank Dr. Michael Kirsch, Institute of Physiology, Klinikum Essen, for valuable advice and helpful discussions. This work was supported by the Deutsche Forschungsgemeinschaft (DFG).

**Supporting Information Available:** Full experimental details on the fluorescence titration, determination of  $\text{IC}_{50}$  values, and enzyme kinetics via Lineweaver–Burk plots as well as native gel electrophoresis. This material is available free of charge via the Internet at <http://pubs.acs.org>.

JA801441J